Multifunctional, Defect Engineered Ru-MOFs: Sorption and Catalytic Properties

Olesia Kozachuk,a Ignacio Luz,b Francesc X. Llabrés i Xamena,b Heshmat Noei,c Max Kauer,c H. Bauke Albada,d Eric D. Bloch,e Bernd Marler,f Yuemin Wang,c* Martin Muhlerc and Roland A. Fischera*

The great diversity and modularity of metal-organic frameworks (MOFs), suggest their competitiveness with traditional porous materials for many applications.[1] Many processes at MOFs involve metal-site/guest-molecule interactions, and thus, the generation and control of reactive, coordinatively unsaturated sites (CUS) within the molecular scaffolds is highly desirable.[2] Generally, MOFs result from the self-assembly of inorganic and organic building blocks in a way that porous and highly ordered crystalline solids are formed: all metal ions are kept by the linkers at fixed positions in a lattice in, ideally, exactly the same coordination environment. CUS are commonly generated when solvent molecules ligating metal centres are removed during activation, for instance at the axial positions of paddle-wheel units in [M3II,II(btc)2] (M = Cu,[3] Mo,[4] Cr,[5] Ni,[6] or Zn;[7] btc3- = benzene-1,3,5-tricarboxylate). Meanwhile, a particular challenge is to enhance the accessibility, even lower the coordination number and thus modify local structure and proximate space with respect to the intrinsic metal ion framework sites by introduction of so-called “structural point defects” originating from partly or even fully missing linker(s) and connections between the metal nodes. The introduction of such defects should, however, not compromise the overall integrity and robustness of the framework.[8]

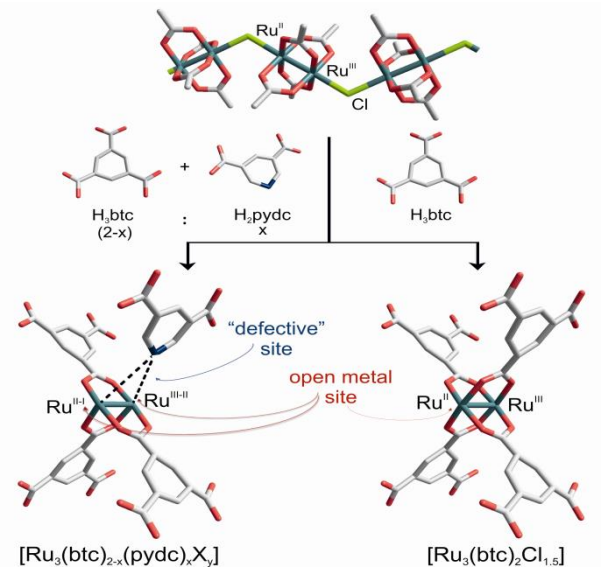

Figure 1. Representation of defect engineered Ru-MOFs D1-D4 (left), [Ru3(btc)2-x(pydc)xXy] (X = Cl, OH, OAc, x = 0.1 (D1), 0.2 (D2), 0.6 (D3), 1 (D4); 0 ≤ y ≤ 1.5), compared to parent [Ru3(btc)2Cl1.5] (right).

The modified CUS are likely to behave different from the parent CUS and are expected to offer novel opportunities for modulating catalytic activity and sorption behaviour of MOFs. The presence of defects in the MOF can have significant effects on the catalytic properties of the

material. These defects can come from an imperfect crystallization of the MOF,[9] but they can also be created in a controlled manner by introducing auxiliary ligands with one missing carboxylate group, as first reported by Farrusseng[10] et al, and later also by De Vos et al.[11] Here, we report on a series of defect engineered variants D1-D4 (Figure 1) derived by framework incorporation of defect generating linkers into the parent Ru(II/III) mixed-valence compound [Ru3(btc)2Cl1.5][12] (1), and we demonstrate multifunctional properties of D1-D4 being enhanced or even absent with respect to 1, ranging from quite unusual CO2→CO dissociative chemisorption ("reduction") at 90 K under ultra high vacuum conditions (UHV) to hydrogen splitting (Ru−H formation) at ambient conditions and related hydrogenation catalysis.

The concept of mixed linker solid solutions[13] was applied to obtain the single-phased [Ru3(btc)2-x(pydc)xXy] (D1-D4) by using mixtures of H3btc and pyridine-3,5-dicarboxylic acid (H2pydc) in the sample synthesis (Figure 1). The (deprotonated) linkers btc and pydc are quite similar in size and structure, just pydc is lacking one carboxylate ligator site. The Cu-analogues [Cu3(btc)2-x(pydc)xXy] (X = NO3-, etc.) were synthesized and studied, previously.[8b] From inspection of the powder X-ray diffraction patterns (PXRD) of the as-synthesized and activated samples it is deduced that D1-D4 are isostructural to the parent single-linker 1 and as well as to [Cu3btc2] (HKUST-1, MOF-199) and its btc/pydc mixed linker variants. The samples exhibit permanent microporosity with values similar to 1 (Figures S3-6, Table S1 in the Supporting Information). While 1 features XPS spin-orbit doublet bands (Ru 3d5/2 and 3d3/2 region) at 281.5 and 285.7 eV, as well as at 282.5 and 286.7 eV characteristic for the Ru(III) and Ru(II) species,[12] an extra doublet at about 280.5 and 284.5 eV appears for D1-D3 (Figures S7, S8; sample D4 was not measured). This new doublet increases gradually in intensity and shifts to 280.0/284.2 eV with increasing the concentration of the defective linker pydc, indicating the presence of the additional Ruδ+ species that are more electron rich compared to Ru(II/III). The formation of reduced Ruδ+ is accompanied by the attenuation of both the Ru(III) 3d bands (at 281.5 and 285.4 eV) and Cl 2p peaks (at 198.4 and 200.0 eV).[12] Along with the C1s and O1s peaks of carboxylate-species at 288.5 and 532.1 eV, respectively, the N1s peak at 400.2 eV is observed, which originates only from pydc. Importantly, on the basis of the O1s data, Ru-oxide impurities are ruled out. These XPS data together with elemental analysis data (Tables S2, S3) and further analytical evidence (Figures S9-S12) support the framework incorporation of pydc resulting in randomly distributed reduced, mixed-valence Ru2-paddle-wheel units with pydc partly replacing the parent btc and with or without (residual) counter-ion(s) or ligands at the axial Ru sites (Figure 1).

CO adsorption isotherms at 298 K were recorded to investigate the effect of the pydc incorporation on the sorption capacity showing an increased uptake. For example, activated D3 reveals a total uptake of 3.88 mmol/g as compared to the parent 1 with a 28 % lower uptake value of 2.8 mmol/g (Figure S13, Table S4). Hence, to gain more detailed insight, the CO adsorption was monitored in situ by UHV-FTIR spectroscopy at low temperature of 90 K (Figures S14, S15).[14] Interestingly, two intense new bands at lower wave numbers are seen at 2000 and 2039 cm-1 for D1-D3, which are absent for the parent 1[12b] and are highly sensitive to the doping level of pydc. These pronounced red-shifted bands are characteristic for various CO species adsorbed on Ru$^{\delta+}$ ($0 < \delta < 2$) species (Table 1). Temperature-dependent CO desorption experiments display fast decrease of the higher-lying bands at 2171 and 2118

cm-1 upon heating and their complete vanishing at 130 K and 190 K indicates the weak binding of (CO)Ru3+ and the relatively stronger binding of (CO)Ru2+, respectively. All further, low-lying bands disappear only at about 280 K, supporting the assignment as CO molecules binding more strongly to electron richer, i.e. reduced Ru□+ sites due to enhanced □-backdonation (Figure S15). Our related theoretical studies on CO binding to the parent 1 have shown,[12b] that the local organization of this "non-defective" framework is not simple, too. Rather, the simultaneous existence of two different types of Ru(II/III) paddle-wheel units, one coordinated with Cl□ at both Ru sites and one with both Ru remaining vacant, provided the best match with the experiment. These reference data also allow to rule out the interpretation of D1-D4 as a physical mixture of parent 1 with various amounts of Ru nanoparticles, because in such a case the intensity ratio of the (CO)Ru3+ and (CO)Ru2+ species as well as their □(CO) frequencies would not depend on the pydc concentration applied during synthesis. Rather, D1-D4 reveal more than two non-equivalent and accessible framework Ru-sites different from 1 (even in case of low-doping with pydc). Notably, related CO adsorption studies monitored by UHV-FTIRS on [Cu3btc2] thin film materials (SURMOFs) showed that about 4% of defective copper sites do exist, that were identified as mixed-valence Cu(I)/Cu(II) paddle-wheels.[8d] Hence, owing to the gradual decrease in over-all anionic charge by increasing pydc doping the response of the framework in reduction of Ru sites is quite plausible.

Table 1. UHV-FTIR data on CO and CO2 adsorption at Ru-species.

Sample	Band (cm^{-1})	Assignment
	CO exposure	
parent *Ru-MOF* (**1**)	2171, 2137	$(CO)Ru^{3+}$, $(CO)Ru^{2+}$
D1	2174, 2133	$(CO)Ru^{3+}$, $(CO)Ru^{2+}$
	2045, **2002**	**$(CO)Ru^{\delta+}$**
D3	2171, 2118	$(CO)Ru^{3+}$, $(CO)Ru^{2+}$
	2039, **2000**	**$(CO)Ru^{\delta+}$**
	CO_2 exposure	
parent *Ru-MOF* (**1**)	2335, 2272	$(CO_2)Ru^{2+}$, $(CO_2)Ru^{3+}$
D1	2335, 2272	$(CO_2)Ru^{2+}$, $(CO_2)Ru^{3+}$
	2039, 2000	**$(CO)Ru^{\delta+}$**
D3	2335, 2272	$(CO_2)Ru^{2+}$, $(CO_2)Ru^{3+}$
	2039, 2000	**$(CO)Ru^{\delta+}$**

Inspired by the above findings we expected unique properties of the defect engineered samples compared to parent 1. First, we studied low temperature CO2 adsorption (UHV-FTIRS). Most surprisingly, after CO2 adsorption on D1-D3 two dominating, low-lying bands were observed at 2039 and 2000 cm-1 matching with (CO)Ru□+ species, and this unambiguously indicates CO2→CO reduction. Importantly, for the parent 1 only bands at 2335 and 2272 cm-1 are observed, which are characteristic for weakly physisorbed CO2, coordinated in linear fashion to Ru-sites. The intensity of these CO2 related bands gradually decreases with increasing pydc doping in the series D1-D3, while a significant enhancement of

the low-lying bands assigned to (CO)Ru⍰+ is observed (Table 1, Figure 2). At this point, it should be noted that dissociative chemisorption of CO2 in the dark was not observed for Ru nanoparticles.[15]

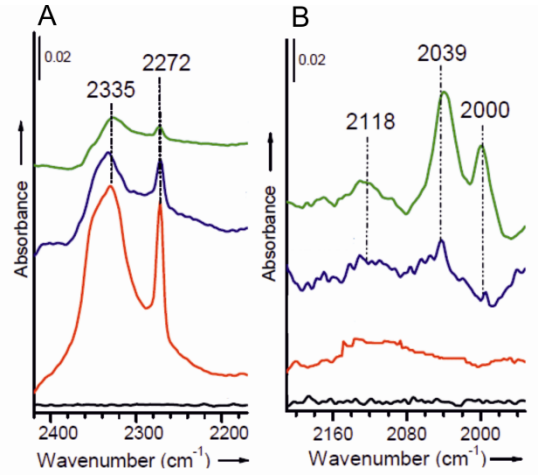

Figure 2. UHV-FTIR spectra (the regions of CO2 (A) and CO (B) vibrations are displayed) obtained at 90 K after exposing the parent 1 (red) and defect engineered D1 (blue) and D3 (green) (representative samples) to CO2 (1x10-4 mbar). Traces (black) represent spectra of 1 prior to the CO2 exposure. Temperature-dependent desorption experiments are given in Figures S16, S17.

Photoinduced reduction of CO2 to CO and other valuable organic molecules has been found on semiconducting nanomaterials (e.g. TiO2, CdS, ZnO) under UV or visible light irradiation.[16] Additionally, electrochemical reduction of CO2 on various metallic electrodes has been reported.[17] For MOFs, however, such a property is rather unprecedented and very few exhibit some activity towards CO2 conversion.[18] Namely for CO2→CO photocatalytic reduction only UiO-67 functionalized with [ReI(dcbpy)(CO)3Cl] (dcbpy=2,2′-bipyridine-5,5′-dicarboxylic acid) was reported.[18a] A number of Ru(II) and Ru(I) molecular complexes are known to be efficient in photo- and electro-catalytic CO2 reduction providing CO or formic acid (or formates) as the products.[19] Since the reaction over D1-D3 takes place also in the dark, we rule out the photochemical pathway. Thus, observing totally inactive parent 1, the CO2→CO at 90 K is likely to be driven by strong interactions with reduced Ruδ+-CUS. Enhanced charge transfer from Ru 3d to the CO2 2πu antibonding orbital possibly yields chemisorbed CO2δ- species that might act as reaction intermediate to finally produce CO. The activation of CO2 could be promoted by pydc due to the basic pyridyl-N sites in the proximity of the reactive Ru sites (possible pyridyl N-oxide formation[20]). In any way, during synthesis of D1-D3 and formation of reduced Ru⍰+, energy is stored in the system to allow the removal of one O-atom from CO2. Unfortunately, we cannot comment on the fate of this oxygen atom.

Ru-complexes have a strong tendency to perform a heterolytic, base-assisted activation of H2, instead of oxidative addition, to generate Ru-hydride species (Ru−H; Scheme 1).[21] Remarkably, D1-D4 show the ability to form such hydride species after H2 treatment as revealed by FT-IR, while fully preserving the structural integrity (Scheme S1, Figures S18-22). In

fact, after heating the samples under p(H2) new bands appear in the characteristic region of Ru−H vibrations at 1956-1975 and 2057-2076 cm-1.[22] This observation prompted us to screen the catalytic properties of the samples and the influence of the defects on the catalytic performance with and without hydrogen pretreatment. Indeed, there is huge variety of reactions, well-known to be catalyzed by Ru: both homogeneous and heterogeneous (like Ru/C or RuO2, etc.).[23] Nevertheless, only few studies were reported on porous solids bearing Ru at the framework nodes and, to the best of our knowledge, none of them on Ru-CUS.[24] In view of the observed tendency of our samples to form Ru−H species, we first investigated the performance as olefin hydrogenation catalysts, using 1-octene as the model compound. To track the influence of the introduced defects the samples D1 with low and D3 with high pydc doping, have been selected. As it can be seen in Figure 3, the parent 1 sample reveals only marginal hydrogenation activity, producing only 12% conversion of 1-octene after 20 h. Introduction of pydc produced a clear increment of the activity, attaining a 1-octene conversion of 50% over sample D3 (30% pydc) after the same reaction time. Meanwhile, along with the expected product octane, a mixture of intermediate products coming from isomerization side reactions were also formed, (E,Z)-2-octene, (E,Z)-3-octene and (E,Z)-4-octene, accounting for ca. 30% of the 1-octene converted (Scheme S2 and Figure S26). This result reveals that some Ru-CUS present in the samples have a certain □-acid character, quite in agreement with the observed behaviour of parent 1 upon CO adsorption at 90 K, as monitored by UHV-FTIR spectroscopy. As expected, the defect engineered samples produced slightly higher amounts of isomerization products than the parent 1, in line with the increased □-binding properties of the defective materials. Interestingly, when the samples were pre-treated in situ in H2 atmosphere at p(H2) = 8 atm and 150 ºC for 2 h before adding the olefin at the reaction temperature, the catalytic performance of the pre-treated materials for olefin hydrogenation dramatically increased (Figure 3), while olefin isomerization side reaction decreased significantly. The enhanced activity and selectivity for olefin hydrogenation against the competing isomerization side reaction is due to Ru−H species efficiently formed during pre-treatment, as revealed by FTIR spectroscopy (see above). Formation of Ru-H is reasonably the rate determining step in a process such as that depicted in Scheme 1. Notably, pydc could possibly assist this heterolytic activation by acting as a suitable base ligand (pyridyl-N site) in proximity of the reactive Ru-centres. Indeed, the rate of 1-octene hydrogenation increased with the doping of pydc, reflecting the extent of hydride species formed during the pre-treatment in each sample. Thus, the time needed to attain full conversion of 1-octene was 3-4 h for the parent 1, 2 h for D1 and less than 1 hour for D3 (Figure 3 insert). In all cases octane was the only product observed at the end of the reaction. Similar hydrogenation results and mechanistic interpretation were reported for Rh(II) carboxylate paddle-wheel MOFs.[25]

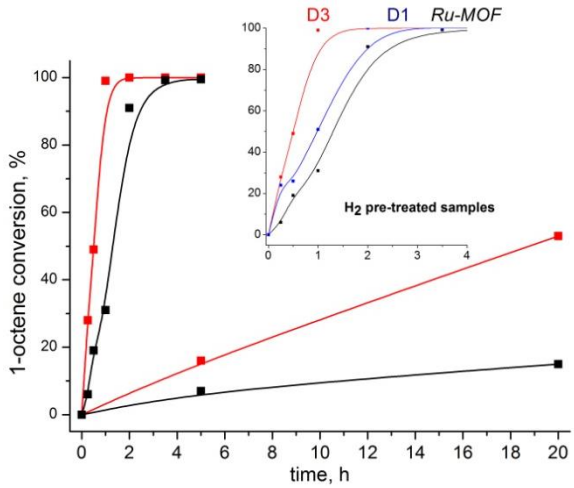

Figure 3. Comparison of the 1-octene conversion in hydrogenation over differently pre-treated samples (see main text): parent Ru-MOF (1) (black), and the defective variants D1 (blue) and D3 (red).

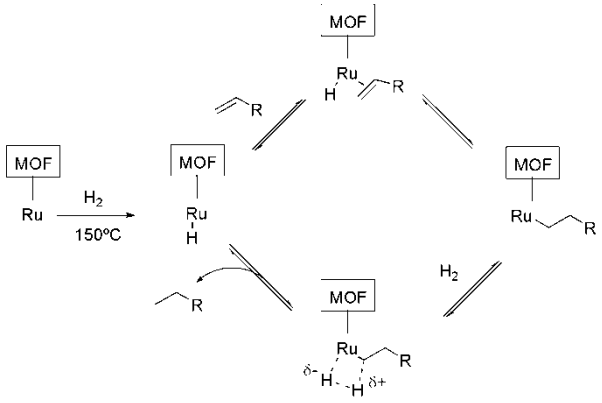

Scheme 1. Conceptual scheme of olefins hydrogenation involving base-assisted heterolytic H2 splitting over defect engineered Ru-MOF samples. Note, that the pydc linker present in D1-D4 (Figure 1) offers a basic pyridyl-N atom in the proximity of the reactive Ru-centres.

Similar to the 1-octene case study, D1-D3 display enhanced performance towards adsorption and interaction with shorter unsaturated hydrocarbons (e.g. ethylene, Figure S27) and serving as catalysts with rather progressive trend upon increasing amount of pydc, for example in hydrogen transfer reactions, such as Meerwein-Pondorf-Verley reduction of carbonyl compounds and isomerization of allylic alcohols to saturated ketones. A more detailed evaluation of the catalytic properties as a function of doping with defective linkers (DLs) is underway and will be reported elsewhere. Let us just anticipate here that the modified Ru-CUS of these materials show multifunctional properties ranging from hydrogenation to oxidation and Lewis acid catalysts.

In summary, we demonstrated the controlled introduction and the characterization of “defective” sites into an isoreticular Ru-analog of HKUST-1. Incorporation of pydc provokes partial reduction of the Ru-sites at the defective paddle-wheel moieties and triggers novel

reactivity, which is absent for the parent [Ru3(btc)2Cl1.5] (1). Thus, we anticipate that other [M3(btc)2] can be similarly modified. The defective linkers (DLs) may be chosen with some variation (Figure 4) and pydc may be regarded as just one representative example. Notably, the electronic modification of CUS (i.e. more electron rich sites) is accompanied with lowered coordination number, i.e. with expanded and functionalized coordination space in the proximity of the modified metal site. This combination of parameters which can be controlled by the choice of DLs (even mixtures of such DLs, S28-S30) and framework incorporation level (i.e. "doping") is likely to yield libraries of a novel kind of multivariate MOFs suitable for automatic screening and property optimization. It may thus be justified to address such kind of mixed-linker (solid solution) derivatives of parent MOFs as being defect engineered at CUS and we like to suggest the acronym DEEMOFs for such kind of samples.

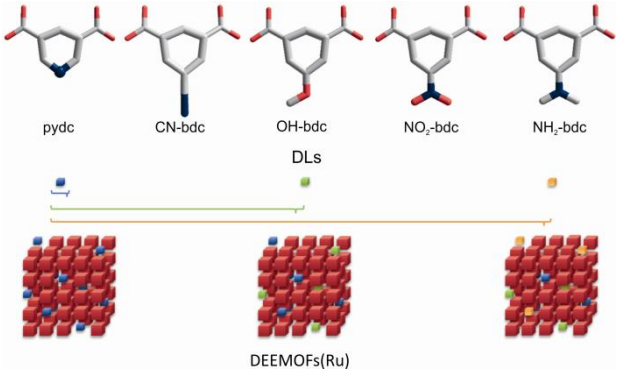

Figure 4. Some defective linkers (DLs) for framework incorporation to yield multivariate defect engineered derivatives of [Ru3(btc)2Cl1.5] (1).

Experimental Section

Synthesis of samples D1-D4, [Ru3(btc)2-x(pydc)xXy] (0.1≤x≤1). The solvothermal synthesis was carried by combining appropriate mixtures of H3btc and H2pydc linkers with 1.5 molar equivalents of [Ru2(CH3COO)4Cl] in deionized water/acetic acid (conc.) for 48 h at 160 °C. The resulting products were filtrated off, washed thoroughly with deionized water and dried, firstly at r.t. with subsequent activation by heating at 150 °C for 24 h under dynamic oil-pump vacuum (ca. 10-3 mbar). Details of the synthesis, applied analytical and characterization methods, full PXRD, FT-IR, TG, SEM, BET, Far-IR, XPS, UHV-FTIR, HPLC, 1H-NMR, elemental analysis (Ru, C, H, N, Cl) sorption and catalytic data of the discussed materials are described in the Supporting Information.

Keywords:ruthenium metal-organic frameworks•structural defects•CO2 reduction•hydrogen splitting•heterogeneous catalysis

[1] a) H. Furukawa, K. E. Cordova, M. O'Keeffe, O. M. Yaghi, Science 2013, 341, 974-98; b) Chem. Soc. Rev. 2009, 38, 1213-1477; c) Chem. Soc. Rev. 2011, 40, 453-1152; d) Chem. Rev. 2012, 112, 673-1268.

[2] a) A. Corma, H. García, F. X. Llabrés i Xamena, Chem. Rev. 2010, 110, 4606-4655; b) T. Uemura, N. Uchida, M. Higuchi, S. Kitagawa, Macromolecules 2011, 44, 2693-2697; c) Y.-Y. Fu, Ch.-X. Yang, X.-P. Yan, Langmuir 2012, 28, 6794-6802.

[3] S. S. Y. Chui, S. M. F. Lo, J. P. H. Charmant, A. G. Orpen, I. D. Williams, Science 1999, 283, 1148-1150;

[4] M. Kramer, U. Schwarz and S. Kaskel, J. Mater. Chem. 2006, 16, 2245-2248.

[5] L. J. Murray, M. Dinca, J. Yano, S. Chavan, S. Bordiga, C. M. Brown, and J. R. Long, J. Am. Chem. Soc. 2010, 132, 7856-7857.

[6] P. Maniam, N. Stock, Inorg. Chem. 2011, 50, 5085-5097.

[7] J. I. Feldblyum, M. Liu, D. W. Gidley, A. J. Matzger, J. Am. Chem. Soc. 2011, 133 (45), 18257-18263.

[8] a) L. Huang, H. Wang, J. Chen, Z. Wang, J. Sun, D. Zhao and Y. Yan,

Microporous Mesoporous Mater. 2003, 58, 105-114; b) S. Marx, W. Kleist, A. Baiker, Journal of Catalysis 2011, 281, 76-87; c) T.-H. Park, A. J. Hickman, K. Koh, S. Martin, A. G. Wong-Foy, M. S. Sanford, A. J. Matzger, J. Am. Chem. Soc. 2011, 133, 20138-20141; d) P. St. Petkov, G. N. Vayssilov, J. Liu, O. Shekhah, Y. Wang, Ch. Wöll, Th. Heine, ChemPhysChem 2012, 13, 2025-2029.

[9] a) C. Chizallet, S. Lazare, D. Bazer-Bachi, F. Bonnier, V. Lecocq, E. Soyer, A. Quoineaud, N. Bats, J. Am. Chem. Soc. 2010, 132, 12365-12377; b) F. X. Llabrés i Xamena, F. G. Cirujano, A. Corma, Microporous Mesoporous Mater. 2012, 157, 112-117.

[10] U. Ravon, M. Savonnet, S. Aguado, M. E. Domine, E. Janneau, D. Farrusseng, Microporous Mesoporous Mater. 2010, 129, 319-329.

[11] F. Vermoortele, B. Bueken, G. Le Bars, B. Van de Voorde, M. Vandichel, K. Houthoofd, A. Vimont, M. Daturi, M. Waroquier, V. Van Speybroeck, C. Kirschhock, D. E. De Vos, J. Am. Chem. Soc. 2013, 135, 11465-11468.

[12] a) O. Kozachuk, K. Yusenko, H. Noei, Y. Wang, S. Walleck, T. Glaser, R. A. Fischer, Chem. Commun. 2011, 47, 8509-8511; b) H. Noei, O. Kozachuk, S. Amirjalayer, S. Bureekaew, M. Kauer, R. Schmid, B. Marler, M. Muhler, R. A. Fischer, Y. Wang, J. Phys. Chem. C 2013, 117, 5658-5666.

[13] A. D. Burrows, CrystEngComm 2011, 13, 3623-3642.

[14] Y. Wang, A. Glenz, M. Muhler, C. Wöll, Rev. Sci. Instrum., 2009, 80, 113108-6.

[15] J. Rasko, Catal. Lett. 1998, 56, 11-15.

[16] a) P. Usubharatana, D. McMartin, A. Veawab, P. Tontiwachwuthikul, Ind. Eng. Chem. Res. 2006, 45, 2558-2568; b) V. P. Indrakanti, J. D. Kubicki, H. H. Schobert, Energy Environ. Sci. 2009, 2, 745-758; c) K. Mori, H. Yamashita, M. Anpo, RSC Advances 2012, 2, 3165-3172.

[17] a) B. Kumar, M. Llorente, J. Froehlich, T. Dang, A. Sathrum, C. P. Kubiak, Annual Rev. Phys. Chem. 2012, 63, 541-69; b) E. E. Benson, C. P. Kubiak, A. J. Sathrum, J. M. Smieja, Chem. Soc. Rev. 2009, 38, 89-99.

[18] a) Ch. Wang, Z. Xie, K. E. de Krafft, W. Lin, J. Am. Chem. Soc. 2011, 133, 13445-13454; b) Yanghe Fu, D. Sun, Y. Chen, R. Huang, Z. Ding, X. Fu, Z. Li, Angew. Chem. Int. Ed. 2012, 51, 3364 -3367.

[19] a) Y. Tsukahara, T. Wada, K. Tanaka, Chem. Lett. 2010, 39, 1134-1135; b) Z. Chen, C. Chen, D. R. Weinberg, P. Kang, J. J. Concepcion, D. P. Harrison, M. S. Brookhart, T. J. Meyer, Chem. Commun. 2011, 47, 12607-12609; c) N. Planas, T. Ono, L. Vaquer, P. Miró, J. Benet-Buchholz, L. Gagliardi, C. J. Cramer, A. Llobet, Phys. Chem. Chem. Phys. 2011, 13, 19480-19484.

[20] S. L. Jain, B. Sain, Chem. Commun. 2002, 1040–1041

[21] a) H. D. Kaesz, R. B. Saillant, Chem. Rev. 1972, 72(3), 231-281; b) D. Sellmann, R. Prakash, F. W. Heinemann, M. Moll, M. Klimowicz, Angew. Chem. Int. Ed. 2004, 43, 1877-1880.

[22] a) X. Wang, L. Andrews, J. Phys. Chem. A 2009, 113, 551-563; b) C. P. Laua, S. M. Nga, G. Jia, Z. Lin, Coord. Chem. Rev. 2007, 251, 2223-2237.

[23] a) K. Yamaguchi, N. Mizuno, Angew. Chem. Int. Ed. 2003, 42, 1480-148; b) F. Su, F. Y. Lee, L. Lv, J. Liu, X. N. Tian, X. S. Zhao, Adv. Funct. Mater. 2007, 17, 1926-1931; c) H. Over, Chem. Rev. 2012, 112, 3356-342; d) H. Miura, K. Wada, S. Hosokawa, M. Sai, T. Kondo, M. Inoue, Chem. Commun. 2009, 4112-4114.

[24] a) R. Tannenbaum, Chem. Mater. 1994, 6, 550-555; b) R. Tannenbaum, J. Molec. Catal. A: Chem. 1996, 107, 207-215.

[25] a) T. Sato, W. Mori, C. N. Kato, T. Ohmura, T. Sato, K. Yokoyama, S. Takamizawa, S. Naito, Chem. Lett. 2003, 32, 854-855; b) T. Sato, W. Mori, C. N. Kato, E. Yanaoka, T. Kuribayashi, R. Ohtera, Y. Shiraishi, J. Catal. 2005, 232, 186-198.